HOSTED BY

ELSEVIER

Research article

Synthesis of zeolite A using the waste of iron mine tailings dam and its application for industrial effluent treatment

Juliana de Carvalho Izidoro[a,*], Michelle Caroline Kim[b], Valentina Ferraraccio Bellelli[b],
Mara Cristina Pane[b], Amilton Barbosa Botelho Junior[a,**], Denise Crocce Romano Espinosa[a],
Jorge Alberto Soares Tenório[a]

[a] *Department of Chemical Engineering, Polytechnic School, University of Sao Paulo. Av. Prof. Luciano Gualberto, travessa 3, No. 380, 05508-010, São Paulo, SP, Brasil*
[b] *Colégio Dante Alighieri, Macro Area of the Sciences of the Nature, Alameda Jaú, 1061, CEP 01420-002, São Paulo, SP, Brazil*

ABSTRACT

In November 2015, a dam from iron mining collapsed, which is considered as the largest environmental accident in Brazil. Over than 50 million m³ were released reaching the Doce River and killed 20 people in Mariana. The literature review shows that the mining tailings can be used as raw material to the synthesis of zeolites, which can be used for the wastewater treatment. The aim of this work was the synthesis of zeolites from the Samarco tailings and its application for the treatment of electroplating effluent. The residue was characterized which identified high-iron content for the synthesis of zeolites. The residue was mixed with NaOH (1:1) and the reaction temperature was evaluated from 350 °C to 650 °C. Then, the material was mixed with aluminum source and the effect of time was evaluated. The zeolite was applied to the wastewater treatment from electroplating industry. Results showed that the synthesis of zeolite A was carried out with a fusion step at 450 °C for 1 h using RAS: NaOH ratio 1:1, and further hydrothermal treatment at 100 °C during 4 h. The zinc removal from the wastewater was up to 98% using 50 mL of the solution, 2.5 g zeolite A, 60min and pH 6.4. The main metals presented in the solution were adsorbed up to 90% by the zeolite synthesized. Zinc adsorption by the zeolite fitted better on Langmuir isotherm. The zeolite was used four times in a row and zinc removal declined 98–68%.

1. Introduction

In 2015 (November 5th), the Fundão dam collapsed, which is the worst environmental disaster in mining. Samarco, a joint venture between BHP Billiton and Vale, produces iron pulp (of 67% iron) which is sent from Mariana (Minas Gerais) to Anchieta (Espírito Santo) by pipes. The waste was deposited in a dam there. Over 50 million cubic meters destroyed 80% of the small village of Bento Rodrigues. After hitting the village, a mud tsunami was released into the Doce River and traveled 600 km to the ocean. The result of the accident was 19 deaths, massive numbers of fish killed, hundreds of thousands of people whose water supply was affected and the destruction of the Doce River (Guerra et al., 2017; Segura et al., 2016).

Over 37 months later, on January 25th, 2019, another dam collapsed in Brumadinho city, also in Minas Gerais state. More than 300 people died (identified and those who disappeared). Also, the Brumadinho disaster destroyed the area's historical and cultural,

environmental and local economy. As a result, the accident is considered to be the worst in mining history (Almeida, Jackson Filho, & Vilela, 2019; Santamarina, Torres-Cruz, & Bachus, 2019). Despite these accidents and the concerns of the government and civilians, there are still more risks of dam collapses in Brazil (Grant, 2019).

According to the Brazilian Mining National Agency (ANM), iron, mostly destined for China, represented 64% of mineral exports in 2018. The Minas Gerais State has 31% of all Brazilian workers from mining companies, and almost half of them work in iron extraction (Departamento Nacional de Produção Mineral, 2018). For this reason, the Brazilian and Minas Gerais State economy are highly dependent on iron extraction.

The tailings generated from iron extraction are stored in dams, such as those which collapsed in Mariana and Brumadinho (Luz, Sampaio, & França, 2010). Due to the risks of dam failures and also the millions of tonnes of tailings stored (Adiansyah, Rosano, Vink, & Keir, 2015; Eduardo et al., 2017; Labonne, 2016; Marta-Almeida, Mendes, Amorim,

Cirano, & Dias, 2016), researchers have been studying different applications for these residues (Fontes et al., 2016; Liu & Poon, 2016). Among the applications, the synthesis of zeolites for wastewater treatment is possible due to its high silica content (Mallapur & Oubagaranadin, 2017).

Zeolites are natural or synthetic materials with common structural features, which have well-defined crystalline structures. These porous materials are composed of hydrated aluminosilicates, which are generally built from tetrahedral MeO_4 units (Me = Si^{+4} or Al^{+3}). The oxygen atom is shared with two atoms of aluminum or silicon, which result in an extended three-dimensional network. The positive charge of silica atoms ($+4$) in the zeolite structure is compensated by oxygens atoms ($+2$); however, if aluminum atoms ($+3$) replace a part of the silica, a negative charge is formed and the ion exchange characteristic of zeolites is obtained (Zagorodni, 2012).

The process of the synthesis of zeolites is composed of the following: steps alkali-fusion, hydrothermal treatment, washing and drying (Mallapur & Oubagaranadin, 2017). Type-A and X zeolites are the most common in industrial applications. Zeolites A are used in wastewater treatment due to their cavity, which make it possible to remove cations presented in a solution. Zeolites X have a cavity large enough to allow the access of organic molecules, which is used in refineries as a catalyst (Izidoro, 2013).

Different pieces of work show the synthesis of zeolites from waste materials (Attari, Bukhari, Kazemian, & Rohani, 2017; Izidoro, Fungaro, & Wang, 2011; Izidoro, Miranda, Guilhen, Fungaro, & Wang, 2018; Wibowo, Rokhmat, Sutisna, Khairurrijal, & Abdullah, 2017). Izidoro, Fungaro, Dos Santos, and Wang (2012) studied the synthesis of zeolites A from coal fly ashes. The SiO_2, Al_2O_3 and Fe_2O_3 content in the residue were 48.4–62.5%, 22.9–32.6% and 3.6–10.2%, respectively (Izidoro et al., 2012). However, the aluminum content in iron mining tailings should be lower or zero, and it is clear that iron content in these residues is higher. As a result, an aluminum source must be added for zeolite synthesis.

The goal of this work was to study the synthesis of zeolites A and its use in the treatment of effluent from the electroplating industry. The sample of iron mine tailings, provided by Samarco and characterized by XRF, was mixed with NaOH (10 g of RAS: 10 g of NaOH) and the temperature of the reaction was evaluated between 350 °C and 650 °C. After the reaction finished, the product was placed in a reaction with an aluminum source with 200 mL of deionized water. The effect of time was studied, in the range of 2–24 h. Analyzes in XRD were made to characterize the products obtained at each step.

The wastewater provided by the electroplating company was characterized by EDXRF. Ion exchange experiments were carried out using 50 mL of the effluent at 25 °C with a stirring speed of 200 rpm. The variables evaluated were the effect of the mass of zeolite, time and pH. Three isotherms of adsorption (Langmuir, Freundlich, and Temkin) were studied. The zeolite reuse was evaluated through five cycles of adsorption. Samples were analyzed in EDXRF.

2. Materials and methods

2.1. Characterization of mine tailings

The sample of the mining tailings from the iron mine was provided by Samarco in February 2018 (Fig. 1). In this study, the residue is called RAS. The residue was characterized by X-ray diffraction (XRD), X-ray fluorescence (XRF), loss on ignition and scanning electron microscope (SEM).

The XRD was performed using Rigaku Multiflex equipment with a copper anode. The scanning speed was 0.06° for 3 s and with 2θ ranging between 10 and 90°. The mineralogical composition was carried out with the aid of the Search-Match computer program and the diffraction pattern database of the International Center for Diffraction Data (ICDD).

The XRF analysis was performed using Bruker equipment, model S8 Tiger. The loss on ignition was carried out at 1020 °C for 2 h. The backscatter electron images were obtained using SEM equipment model

Fig. 1. Sample of iron mining tailings provided by the Samarco company in February 2018.

Philips XL-30 at 15 kV. The samples were placed in metallic support and covered with a thin layer of gold to make them conductive before SEM analysis.

2.2. Synthesis of zeolites A

The synthesis of zeolites from tailings, with the use of sodium hydroxide as a caustic agent, has already been discussed in the literature (Izidoro et al., 2011, 2012, 2018; Izidoro, Fungaro, Abbott, & Wang, 2013). Such synthesis was possible due to the high-silica content in RAS. However, there is no literature for the synthesis of zeolites with high-iron content. For this reason, theRAS:NaOH ratio at 1:1 (10 g of RAS: 10 g of NaOH) was studied at the temperatures of 350,450, 550 and 650 °C. The most important parameter for zeolite synthesis is the quartz phase (SiO_2) decrease which forms sodium silicate (Na_2SiO_3).

Sodium aluminate was used as an aluminum source and added after cooling the mixture of RAS and NaOH at room temperature for 1 h. The kinetics reaction to hydrothermal treatment was studied for between 2 and 24hr and mixed with 200 mL of deionized water. After the experiment, the mixture was cooled and filtrated and washed with deionized water. The solid phase was dried in an oven at 100 °C for 24 h. Samples of each experiment were analyzed in SEM and XRD. A particle size analysis was performed with the zeolite obtained in better conditions.

2.3. Adsorption experiments for pollutant removal

A waste sample from the electroplating process with zinc was used in adsorption experiments. The wastewater (pH 6.4) was characterized using Energy-dispersive X-ray spectroscopy (EDXRF). The main metals analyzed for adsorption experiments were titanium, chromium, iron, cobalt, copper, and zinc. All adsorption experiments were carried out at 25 °C with a stirring speed of 200 rpm. The quantity of the mass of zeolite studied was 0.5–2.5 g with 50 mL of solution. The effect of time was studied for between 30 and 120 min with 0.5 g of zeolite and 50 mL of solution.

The effect of pH on adsorption experiments with an ion exchange reaction (Botelho Junior, Dreisinger, & Espinosa, 2019; Zagorodni, 2012), which in the present study was evaluated in the pH range 2.0–5.0 and the results were compared with metals adsorption at 6.4 (initial pH value), is important. The hydrogen ions (H^+) compete with the metals in the solution in an ion-exchange reaction. In high concentrations (acidic pH) there is more H^+ for the reaction, which decreases the absorption of the metals by the zeolite (Botelho Junior, Vicente, Espinosa, & Tenório, 2019, a, 2019, b; Zagorodni, 2012).

Three isotherms were studied: Langmuir, Freundlich, and Temkin. Equation (1) shows the Langmuir isotherm model (homogenous adsorption system), where Q_{max} (maximum monolayer adsorption

capacity of adsorbent, mg/g) and K_L (Langmuir constant, L/mg). Equation (2) shows the Freundlich isotherm model (heterogeneous system), where K_f is the Freundlich constant (mg/g) and n (dimensionless) is the heterogeneity factor (Botelho Junior, Vicente, Espinosa, & Tenório, 2019a). The Temkin isotherm model (Equation (3)) supposes that the heat of the adsorption of the molecules on the surface of the adsorbent decreases linearly instead of logarithmically, opposing Freundlich's model (Wibowo, Rokhmat, Sutisna, & Abdullah, 2017).

$$\frac{C_e}{q_e} = \frac{1}{Q_{\max}K_L} + \left(\frac{C_e}{Q_{\max}}\right) \tag{1}$$

$$\log q_e = \log K_f + \frac{1}{n}\log C_e \tag{2}$$

$$q_e = B\ln A + B\ln C_e \tag{3}$$

Adsorption experiments with five cycles were performed according to the optimal conditions of time, the mass of zeolite and pH. After the adsorption reaction, the zeolite was separated from the solution by filtration, washed using deionized water and dried in an oven at 25 °C for 24 h. Then, a new cycle was carried out. The entire aqueous phase was analyzed using EDXRF. Fig. 2 shows the flowsheet of the experiments performed.

3. Results and discussion

Table 1 shows the chemical composition of the residue from iron

Fig. 2. Flowsheet of the synthesis of zeolites A.

Table 1
Chemical composition of residue from iron mining analyzed by XRF.

Component	Percentage
SiO_2	79.3
Fe_2O_3	19.3
Al_2O_3	0.46
Cr_2O_3	0.15
MgO	0.04
SO_3	0.04
P_2O_5	0.03
K_2O	0.03
CaO	0.03
TiO_2	0.02
MnO	0.02
Na_2O	0.01
Cl, CuO, ZnO, SrO, ZrO_2, Nb_2O_5, BaO, La_2O_3, CeO_2 and PbO	<0.01
Losson ignition (%)	0.5

mining. The sample was analyzed by XRF. The main component is silicon, followed by iron, aluminum, and chromium. The removal of impurities from iron ore is usually carried out by flotation, and a part of the iron goes with the residue, which justifies the presence of it in RAS (Almeida et al., 2018).

As the main component for the synthesis of zeolites is silicon, the residue can be used for the synthesis of zeolite. However, the high-iron content makes the synthesis of zeolites A different. In addition, the presence of aluminum can be used as an external source of zeolite synthesis.

Fig. 3 shows the XRD analysis of RAS. The main mineral phase was determined as quartz (Q), which is the main component for zeolite A synthesis. The scanning electron microscope (SEM) images of RAS are shown in Fig. 4. The morphology of the residue is irregular with different sizes. The different crystal setting of quartz is responsible for the particles of irregular size (Almeida et al., 2018; Izidoro et al., 2012).

3.1. Synthesis of zeolite A

The effect of temperature on zeolite A synthesis was studied. The temperatures tests were performed at 350 °C, 450 °C, 550 °C, and 650 °C. The mass of RAS and NaOH was 10 g (RAS:NaOH = 1:1). Fig. 5 depicts the XRD of the residue and zeolites obtained at the temperatures studied. The quartz peaks identified in RAS (Fig. 3) decrease when temperate increases.

At 450 °C, the number of peaks of quartz is lower than at 350 °C. However, this number slightly increased at 550 °C and decreased during the fusion step carried out at 650 °C. This may be a result of quartz polymorphism, which changes the crystal structure when heated at
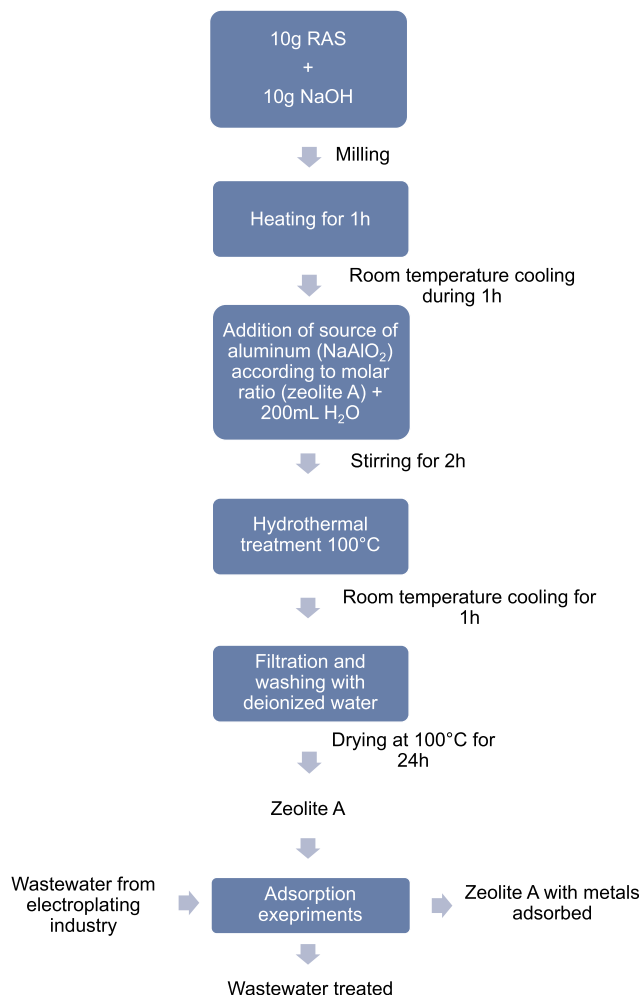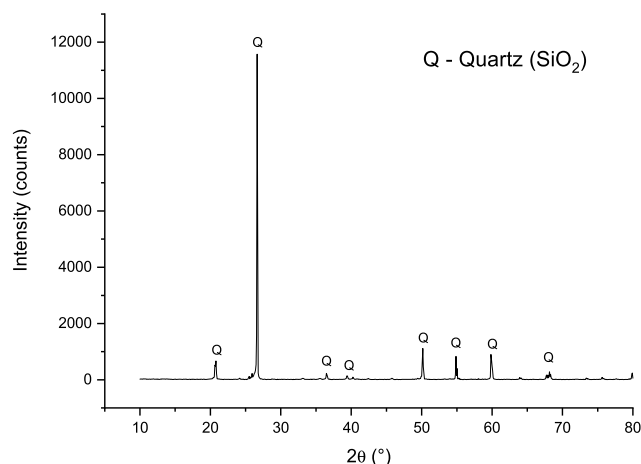

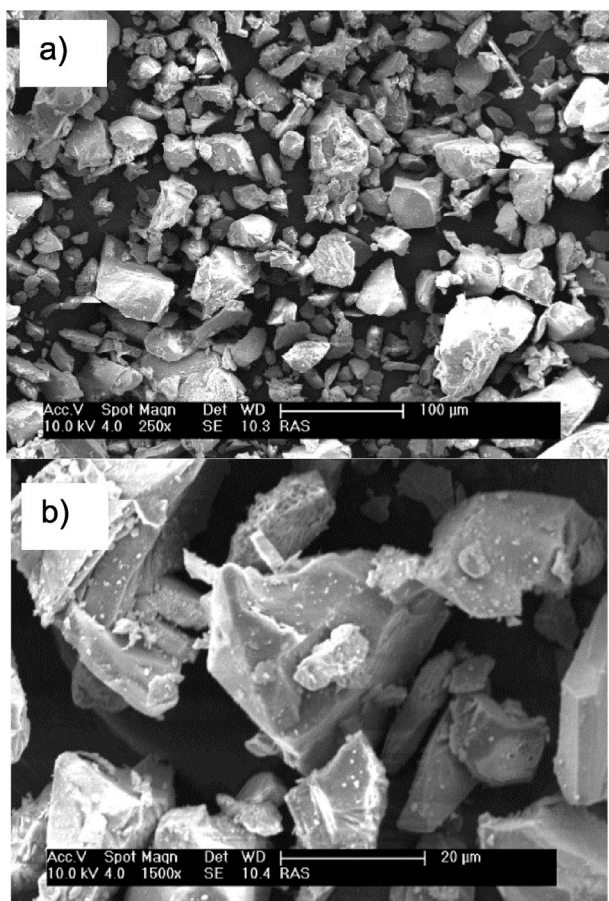**Fig. 3.** X-ray diffraction of the residue from iron mining – RAS.

Fig. 4. Scanning electron microscope (SEM) micrographs of the RAS: a) 250x and b) 1500x.

different temperatures (Attari et al., 2017; Izidoro et al., 2012, 2013; Petrov & Michalev, 2012).

As a result, the temperature choice for the following experiments is

450 °C, which is sufficient for the formation of sodium silicate structures. The structure is soluble in water and leaves the silicate available to form zeolite A. The effect of time on zeolite A synthesis was also studied. After the reaction at 450 °C, the product obtained was cooled at room temperature and mixed with deionized water and aluminum. The mixture was heated to 100 °C and for the following periods of studied time: 2, 3, 4, 5, 6, 12, 18 and 24 h. Fig. 6 shows the XRD of the tests performed for 2–5 h.

An experiment performed for 2 h (TH 2) quartz as the main phase. Zeolite A, hematite and sodium aluminosilicate hydrate were also present. The results obtained after 2 and 3 h showed an amorphous phase (25–30 2θ angles). Experiments carried out for 3 (TH 3), 4 (TH 4) and 5 (TH 5) hours resulted in high-purity zeolites A with traces of silicon compounds, as sodium aluminosilicate hydrate (TH 3) and quartz (Q).

The XRD obtained for experiments performed for 6, 12, 18 and 24 h are shown in Fig. 7. The main phase presented in all results is zeolite A, which was similar to the zeolites obtained for 4 and 5 h. Phases of sodium silicate and quartz were also detected.

Fig. 8 shows the SEM image of experiments carried out for 2–5 h. The zeolites synthesized for 4 and 5 h present a cubic structure, which is characteristic of zeolite A. However, experiments carried out for 2 and 3 h resulted in zeolites with no defined form, which indicates that shorter hydrothermal treatment is insufficient for zeolite A formation. The morphology of experiments performed for 6–24 h was similar to the 4 and 5 h experiments. Accordingly, the reaction time of 4 h was chosen to be used for wastewater treatment experiments.

Fig. 9 shows the particle size distribution of zeolite A synthesized using the best parameters: RAS:NaOH ratio of 1:1 at 450 °C for 1 h and, then, a reaction with an aluminum source at 100 °C for 4 h. The most particles have a size of 10 μm (2–50 μm range). The D10, D50 and D90 values are, respectively, 2.167 μm, 12.367 μm and 90.091 μm.

3.2. Adsorption experiments

Adsorption experiments were carried out using a sample of the real effluent. Table 2 shows the concentrations of the elements presented in a waste sample from the electroplating industry. The main elements are phosphorous (1130 mg/L), sulfur (2420 mg/L) and zinc (2540 mg/L).
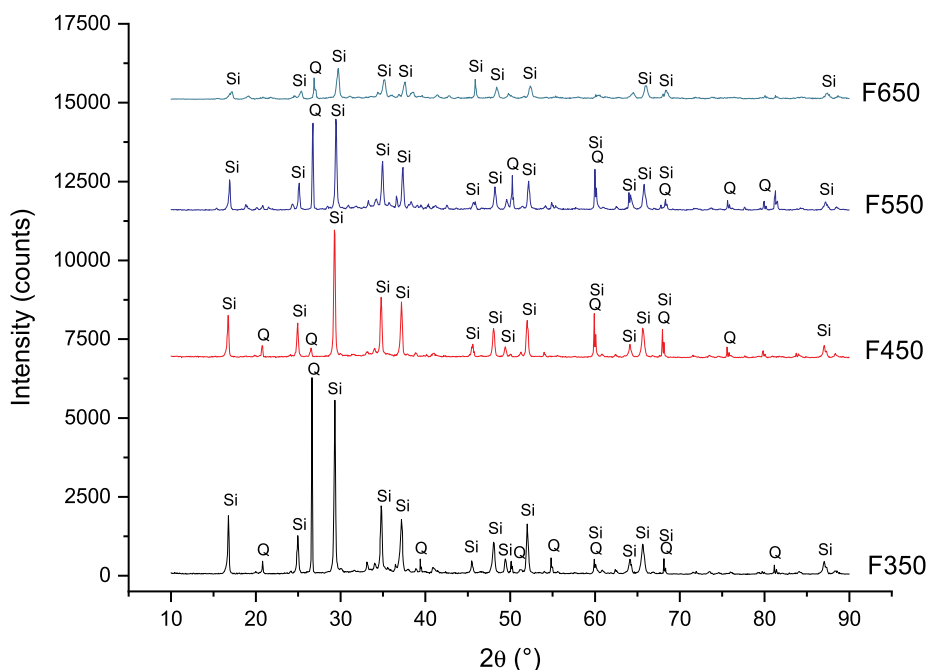

Fig. 5. X-ray diffraction of the zeolites synthesized at different temperatures (Q = Quartz: SiO_2; Si = Sodium silicate: Na_2SiO_3).
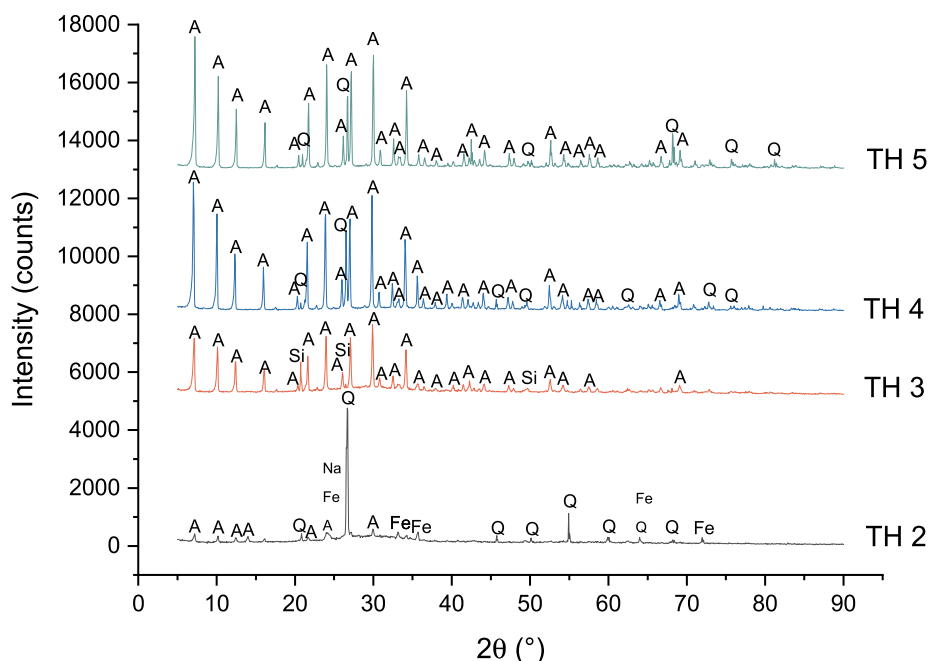
Fig. 6. X-ray diffraction of the zeolites synthesized for 2–5 h (Q = Quartz: SiO_2; A = zeolite A: $Na_2Al_2Si_{1.85}O_7.7.5H_2O$; Na = Sodium aluminosilicatehydrate: $Na_3(H_2O)$, Fe = Hematite: Fe_2O_3; Si = Sodium silicate: Na_2SiO_3).
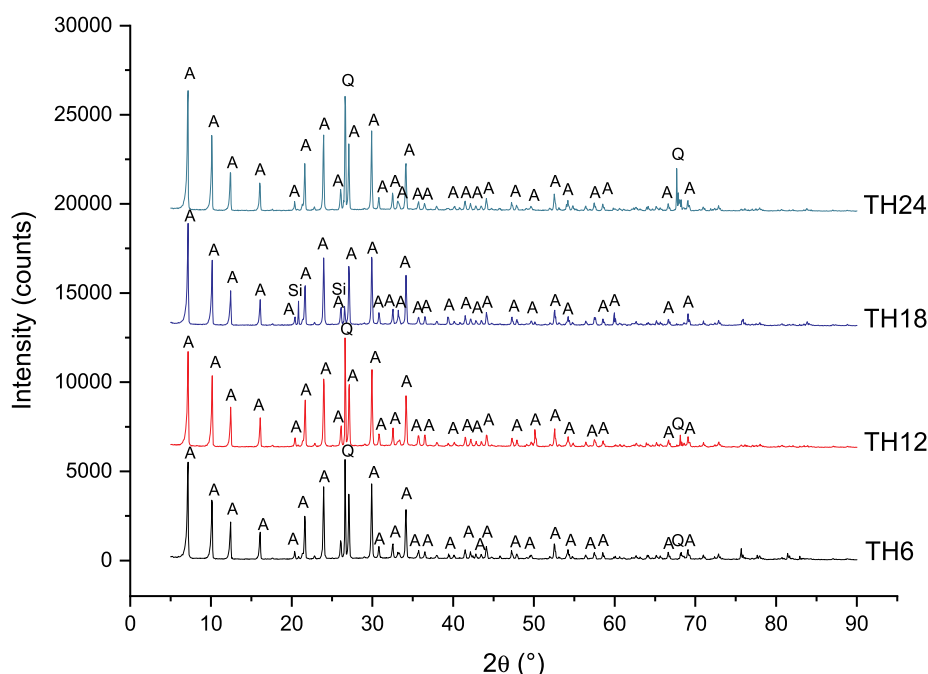

Fig. 7. X-ray diffraction of the zeolites synthesized for 6–24 h ((Q = Quartz: SiO_2; A = zeolite A: $Na_2Al_2Si_{1.85}O_7.7.5H_2O$; Si = Sodium silicate: Na_2SiO_3).

Metals such as titanium (14.8 mg/L), chromium (4.7 mg/L), iron (35.5 mg/L), cobalt (16.1 mg/L) and copper (6.4 mg/L) are also present in the solution. Zinc and these metals were the focus of this piece of work.

Fig. 10 shows the zinc speciation diagram, varying the pH from 0.0 to 14.0. The diagram was elaborated using Hydra-Medusa software. The zinc is present in the solution as Zn^{+2} (100%) in the pH range 0.0–5.0. In pH above 5.0, $ZnOH^+$ begins to form and Zn^{+2} concentration decreases. At pH 7.5, the fraction of both is equal.

At pH 7.0, the $Zn(OH)_2$ begins to form and its fraction stays at 60% in pH above 9.2 and then decreased at pH 11.5. The precipitation of zinc begins at pH 9.0 and reaches its maximum fraction at pH 10.33,

and then decreases. At pH 10.33, zinc is presented as $Zn(OH)_2$, $Zn(OH)_3$–$ZnOH^-$, and as a solid phase ZnO.

For this reason, zinc removal by precipitation is not possible completely. At pH 10.33, approximately 31% of zinc compounds would be oxide in a solid phase (ZnO), 62% as $Zn(OH)_2$ and 7% as $ZnOH^+$ and Zn $(OH)_3^-$, as seen in Fig. 10. Additionally, the pH control and the process costs to change the pH from 6.4 to 10.3 might be high and make the process unfeasible. Also, the treatment of hydroxide precipitatesis not easy due to their binding with water by a hydrogen bond, which makes the solid/liquid separation forming a gelatinous and voluminous precipitate difficult (Jackson, 1986).
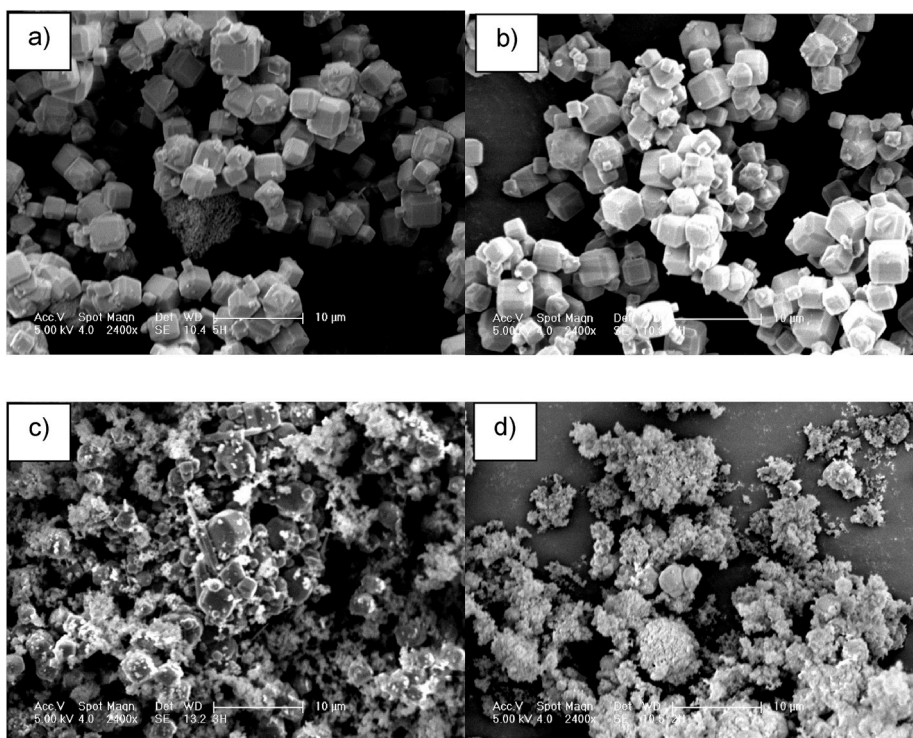
Fig. 8. SEM images of the experiments performed for a) 5, b) 4, c) 3 and d) 2 h.
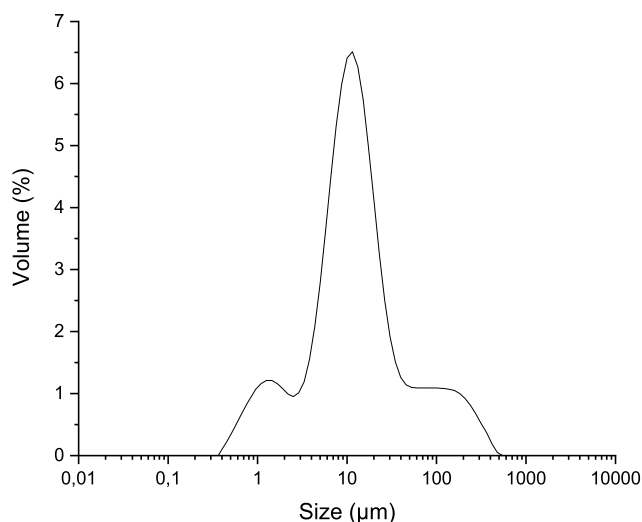

Fig. 9. Particle size analysis of zeolite A synthesized at 450 °C with RAS: NaOH ratio of 1:1 and with a reaction time with the aluminum source of 4 h.

Table 2
Concentration of metals present in wastewater from the electroplating industry.

Elements	Concentration (mg/L)
Mg	82.5
Si	664.3
P	1130.0
S	2420.0
Cl	543.6
K	219.4
Ca	895.5
Ti	14.8
Cr	4.7
Fe	35.5
Co	16.1
Cu	6.4
Zn	2540.0
Ba	19.6

3.2.1. The effect of quantity zeolites on metal adsorption

Experiments were performed in erlenmeyer 250 mL with 50 mL of wastewater at 25 °C and 200 rpm. The adsorption reaction was carried out for 120 min. The mass of zeolites A studied was 0.5 g, 1.0 g, 1.5 g, 2.0 g, and 2.5 g. Fig. 11 depicts the percentage of metal removal from the industrial effluent. Titanium and chromium removal increased from 89% to 83% using 0.5 g to 100% and 96% using 2.5 g, respectively. Iron removal remained the same (95%).

The increase of the quantity of zeolite A in contact with metals in solution raise the number of activites of the adsorbent. Cobalt removal was 1%, with 0.5 g of zeolite A, and increased to 99%, with 2.5 g. Copper adsorption also reached its maximum with 2.5 g of zeolite.

Zinc removal, the main metal in the solution, increased from 35% using 0.5 g to 96% using 2.0 g of zeolite. The adsorption of zinc was

98% with 2.5 g of the adsorbent. Despite titanium, chromium, iron, and zinc reaching their maximum using 2.0 g, the adsorption of cobalt and copper reached their maximum values using 2.5 g of zeolite A.

3.2.2. The kinetic effect on the adsorption process

The effect of time on metal adsorption was studied using the following time periods: 30 min, 60 min, 90 min, and 120 min. The zeolite (0.5 g) was placed in contact with 50 mL of the solution in erlenmeyer 250 mL. The flask was shaken at 200 rpm and at a temperature of 25 °C. The pH of the solution did not change (pH 6.4).

The percentage of metals adsorbed is presented in Fig. 12. The adsorption of iron, cobalt, and titanium reached equilibrium after 30 min. The chromium removal was 55%, 72%, 70% and 82% after 30 min, 60 min, 90 min, and 120 min, respectively. Copper recovery slightly increased during the reaction – from 14% at 60 min to 25% in 120 min. For this reason, the reaction time of 60 min and mass of zeolite of 2.5 g was adopted in order to study the effect of pH and cycles of use.
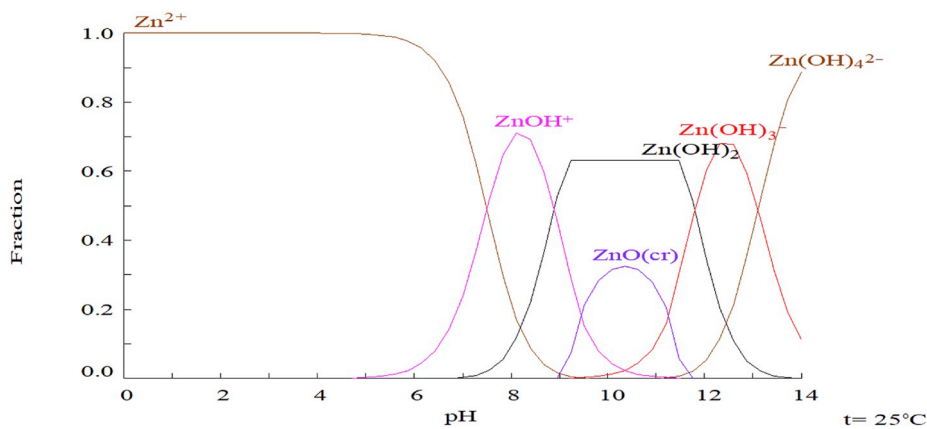
Fig. 10. Zinc speciation diagram varying the pH from 0.0 to 14.0 elaborated using Hydra Medusa software.
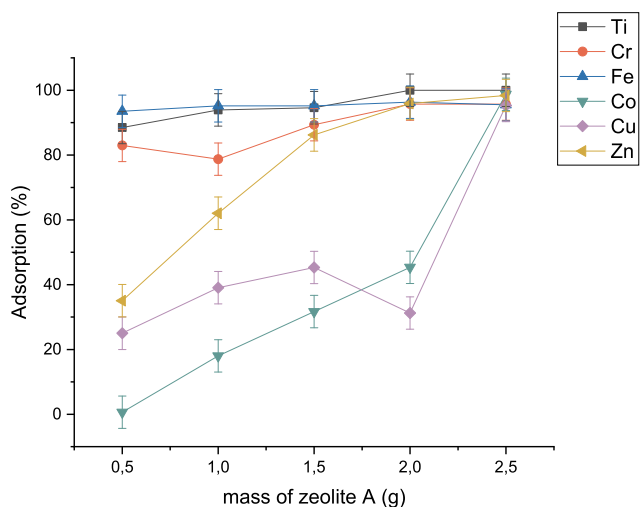

Fig. 11. Effect of the mass of zeolite A on titanium, chromium, iron, cobalt, copper and zinc removal from the electroplating industry.
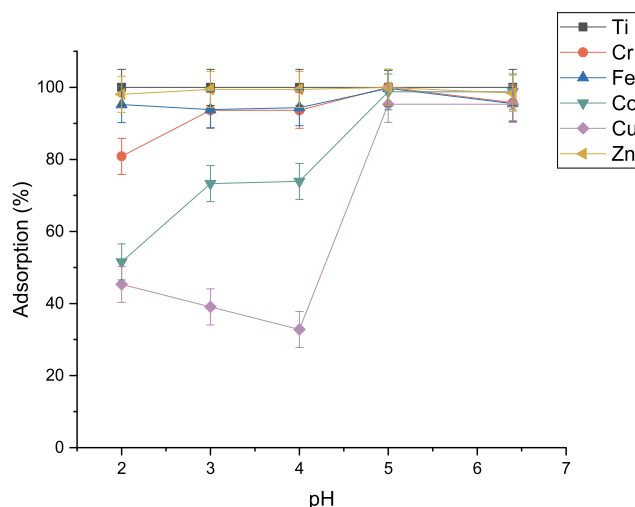

Fig. 13. Effect of pH on titanium, chromium, iron, cobalt, copper and zinc removal from the electroplating industry.
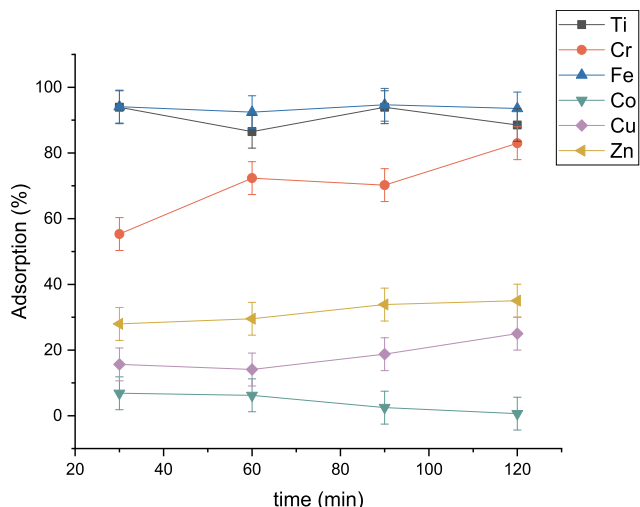

Fig. 12. Effect of time on titanium, chromium, iron, cobalt, copper and zinc removal from the electroplating industry.

3.2.3. The pH influence on pollutant removal

The effect of pH on metal adsorption was studied with 2.5 g of zeolite for 60min. The pH values studied were 2, 3, 4 and 5, in which the results of metal removal were compared with an experiment performed at 6.4. At pH 7.0 (as seen in Fig. 10) a part of the zinc

precipitates. The results are presented in Fig. 13.

The adsorption process is influenced by the pH of the solution. The negative charges of the surface cause the zeolite to attract positive ions and repulse negative ions (Wibowo et al., 2017). As a result, in acidic pH, the H^+ ions compete with the metals presented in the solution for the zeolite surface. Therefore, the removal of cations should increase with the pH of the solution.

Titanium, iron and zinc removal were not affected by the pH of the solution. Cobalt adsorption increased from 52%, at pH 2.0, to 73% at pH 3 and 4, and then to 99% at pH 5 and 6.4. A similar effect was observed for copper removal. Chromium removal increased from 81% at pH 2.0–94% at pH 3 and then reached equilibrium. According to the results, there is no reason to change the pH of the effluent for metal removal. The industrial process of wastewater treatment from electroplating can be carried out without pre-treatment, in a batch or, preferably, in a continuous flow.

The decreased copper adsorption in the pH range 2–4 might be caused by the competition between copper ions and the numerous ions in the solution. Indeed, increased pH also led to an increase in metal adsorption, mainly cobalt and chromium, while copper adsorption declined. This indicated that the zeolite synthesized might have the following order of selectivity, among the metals presented in Fig. 13: Ti > Zn > Fe > Cr > Co > Cu. According to the data provided by Jackson (1986), copper precipitation begins at pH 4, at the concentration shown in Table 2 (Jackson, 1986). For this reason, the copper removal in the pH range 5–6.5 is caused by precipitation as hydroxide $(Cu(OH)_2)$.
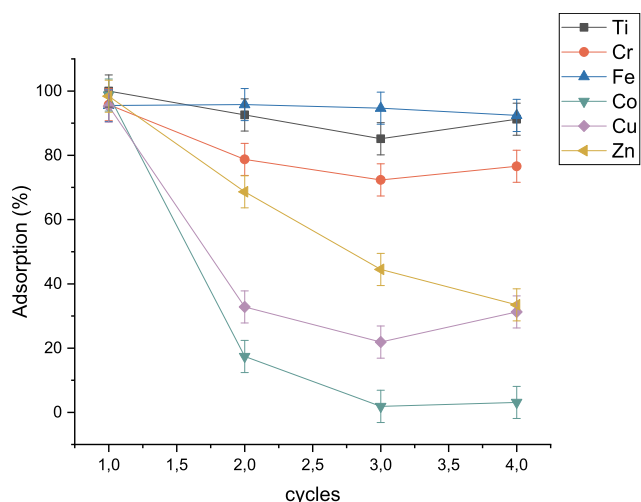
Fig. 14. The effect of cycles of use on titanium, chromium, iron, cobalt, copper and zinc removal from the electroplating industry.

3.2.4. The reuse of zeolite on metals removal

The cycles of use were evaluated using the same zeolite four times. The zeolite (2.5 g) was placed in contact with 50 mL of solution. After 60 min, the mixture was filtrated, the zeolite washed with deionized water and dried in an oven at 60 °C for 24 h. Then, this zeolite was placed in contact with the industrial effluent. The results are presented in Fig. 14.

Titanium and iron removal were similar in all cycles. Chromium, cobalt and copper removal declined from 95%, 98% and 95%–76%, 3% and 21%, respectively. Comparing the concentration of these metals in wastewater (lower than 40 mg/L), it was expected that the reuse of zeolites A would not affect the adsorption of the metal. However, the solution has different concentrations of elements. Chromium and copper are presented in the solution at 4.7 mg/L and 6.4 mg/L. However, zinc and calcium are presented at 2540 mg/L and 895.5 mg/L, respectively. Then, as all elements are adsorbed by the zeolite and occupy the active sites, the adsorption efficiency is decreased.

The percentage of zinc removal declined from 98% (cycle 1) to 68% (cycle 2). The zinc removal was, respectively, 44% and 33% in cycle 3 and cycle 4. As a result, in a batch process, it can be verified that the removal of metal decreased after the first cycle. However, for industrial applications, wastewater treatment can be carried out as a continuous
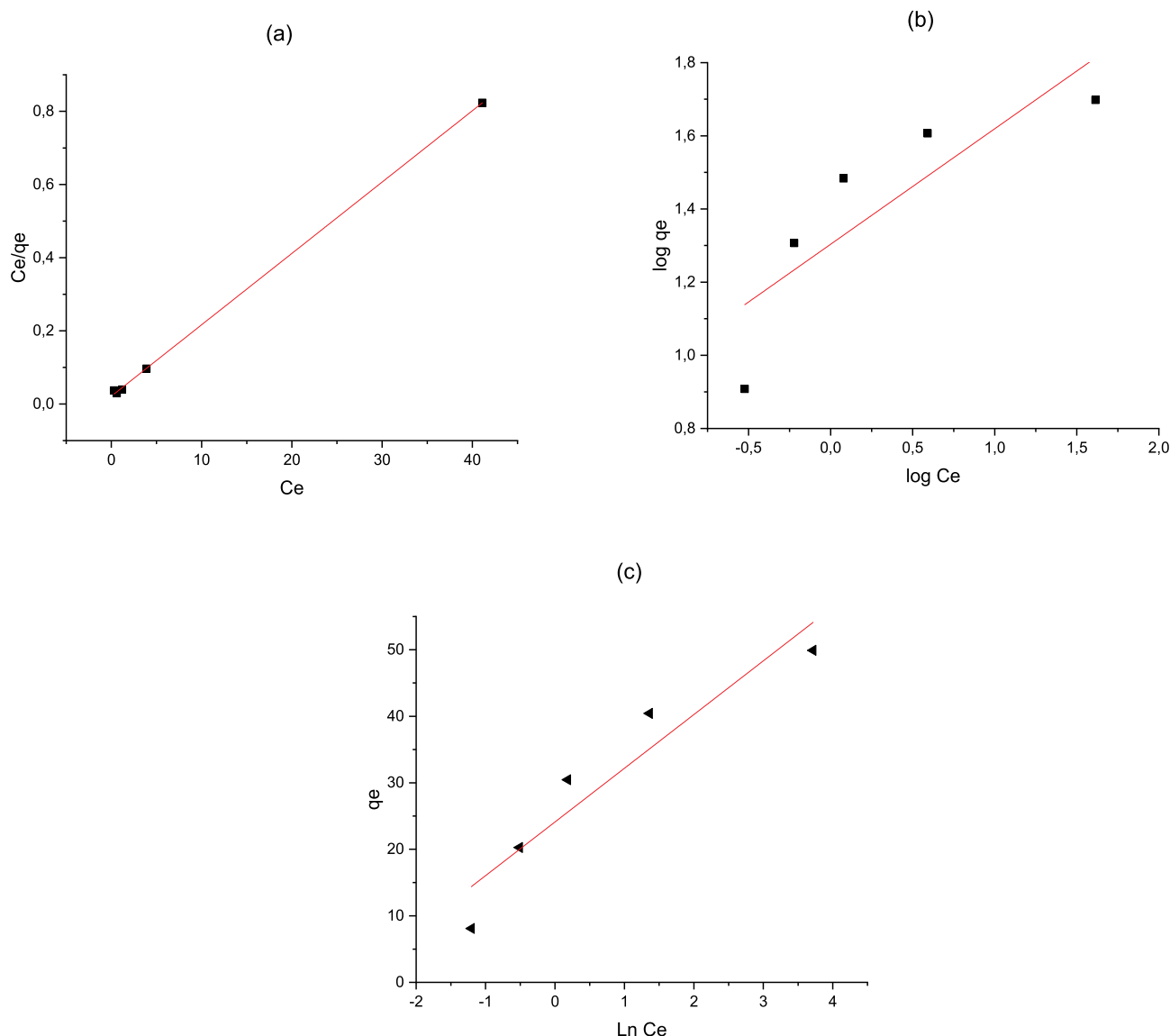

Fig. 15. (a) Langmuir, (b) Freundlich and (c) Temkin isotherms evaluated for zinc adsorption.

Table 3
The calculated Langmuir, Freundlich and Temkin parameters for zinc adsorption with a concentration range of 2540–406.4 mg/L.

	Langmuir			Freundlich			Temkin	
	Q_{max} (mg/g)	K_L (L/mg)	R^2	K_f (mg/g)(mg/L)$^{1/n}$	n	R^2	A	R^2
Zinc	51.256	2391.8	0.99971	3.6822	3.1672	0.71923	19.821	0.89587

process, which enables the treatment of a higher volume of effluent than in the batch process (Inamuddin, & Luqman, 2012).

3.2.5. Langmuir, Freundlich and Temkin isotherms for zinc adsorption

Three adsorption isotherms were studied. The Langmuir, Freundlich and Temkin isotherms were evaluated for zinc adsorption. Experiments were performed using the effluent and the concentration of zinc was decreased: 2540, 2032, 1534, 1016 and 406.4 mg/L. The results are shown in Fig. 15.

Zinc adsorption fitted better for Langmuir ($R^2 = 0.99$) than Freundlich ($R^2 = 0.72$) and Temkin ($R^2 = 0.90$), which indicates that zinc adsorption is by a homogeneous system and a monolayer of the ions is formed in the solid surface, while the Freundlich model assumes physical adsorption on heterogeneous surfaces and the Temkin model assumes that the adsorption is characterized by a uniform distribution on the binding energies (Botelho Junior et al., 2019a; Inamuddin, & Luqman, 2012).

Attari et al. (2017) studied the synthesis of zeolite A from coal fly ash for mercury removal. Experiments showed that mercury adsorption fitted better with Freundlich isotherms (Attari et al., 2017). Table 3 depicts the model parameters calculated for this present study. The K_L calculated for the zinc adsorption by zeolite A is 2391.8 L/mg and the Q_{max} calculated is 51.256 mg/g. The Langmuir isotherm indicates that a monolayer of the zinc is formed when the surface of the zeolite reaches saturation. The value of Q_{max} indicates the practical limiting adsorption capacity when the surface of the zeolite is saturated by zinc.

The iron mining industries are responsible for the production of tonnes of daily waste. The reuse of these materials can help to avoid disasters which affect the environment and the general population. The accidents in Mariana (2015) and Brumadinho (2019) in Minas Gerais State (Brazil) caught the attention of the whole world and highlighted the risks of the extraction process. For this reason, different applications for the residues generated must be studied and developed.

4. Conclusion

The goal of this work was to study the synthesis of zeolites A from iron mining tailings and its application for wastewater treatment from the electroplating industry. The mining waste is composed mainly of silicon (SiO_2_79.3%) and iron (Fe_2O_3 – 19.3%). The best option zeolite A synthesis was a RAS: NaOH ratio of 1:1 with the fusion step at 450 ˚C for 1 h and, then, reaction with an aluminum source at 100 ˚C for 4 h. The zeolite synthesized was tested for effluent treatment from the electroplating industry. The wastewater was mainly composed of zinc (2540 mg/L). Results of adsorption experiments showed that the zinc removal was at its maximum (98%) using 50 mL of the solution, 2.5 g zeolite A, 60min and pH 6.4. The zinc removal decline from 98% at the first use of the zeolite to 68% after the fourth use. Zinc adsorption fitted better with the Langmuir isotherm than the Freundlich and Temkin isotherms.

Ethical statement

Authors state that the research was conducted according to ethical standards.

Declaration of competing interest

None declared.

References

Adiansyah, J. S., Rosano, M., Vink, S., & Keir, G. (2015). A framework for a sustainable approach to mine tailings management: Disposal strategies. *Journal of Cleaner Production, 108*, 1050–1062. https://doi.org/10.1016/j.jclepro.2015.07.139.

Almeida, I. M. de, Jackson Filho, J. M., & Vilela, R. A. de G. (2019). Razões para investigar a dimensão organizacional nas origens da catástrofe industrial da Vale em Brumadinho, Minas Gerais, Brasil. *Cadernos de Saúde Pública, 35*(4), https://doi.org/10.1590/0102-311x00027319.

Almeida, C. A., Oliveira, A. F. de, Pacheco, A. A., Lopes, R. P., Neves, A. A., & Lopes Ribeiro de Queiroz, M. E. (2018). Characterization and evaluation of sorption potential of the iron mine waste after Samarco dam disaster in Doce River basin – Brazil. *Chemosphere, 209*, 411–420. https://doi.org/10.1016/j.chemosphere.2018.06.071.

Attari, M., Bukhari, S. S., Kazemian, H., & Rohani, S. (2017). A low-cost adsorbent from coal fly ash for mercury removal from industrial wastewater. *Journal of Environmental Chemical Engineering, 5*(1), 391–399. https://doi.org/10.1016/j.jece.2016.12.014.

Botelho Junior, A. B., Dreisinger, D. B., & Espinosa, D. C. R. (2019). A review of nickel, copper, and cobalt recovery by chelating ion exchange resins from mining processes and mining tailings. *Mining, Metallurgy & Exploration, 36*(1), 199–213. https://doi.org/10.1007/s42461-018-0016-8.

Botelho Junior, A. B., Vicente, A. A., Espinosa, D. C. R., & Tenório, J. A. S. (2019). Effect of iron oxidation state for copper recovery from nickel laterite leach solution using chelating resin. *Separation Science and Technology*. https://doi.org/10.1080/01496395.2019.1574828.

Botelho Junior, A. B., Vicente, A. A., Espinosa, D. C. R., & Tenório, J. A. S. (2019). Recovery of metals by ion exchange process using chelating resin and sodium dithionite. *Journal of Materials Research and Technology, 8*(5), 4464–4469. https://doi.org/10.1016/j.jmrt.2019.07.059.

Departamento Nacional de Produção Mineral (2018). Informe mineral 1o/2018. Retrieved from http://www.anm.gov.br/dnpm/publicacoes/serie-estatisticas-e-economia-mineral/informe-mineral/publicacoes-nacionais/informe_mineral_1_2018.pdf.

Eduardo, L., Gomes, D. O., Barreto, L., Sá, F., Rodrigues, R., & Fraga, A. (2017). The impacts of the Samarco mine tailing spill on the Rio Doce estuary, Eastern Brazil. *Marine Pollution Bulletin, 120*(1–2), 28–36. https://doi.org/10.1016/j.marpolbul.2017.04.056.

Fontes, W. C., Mendes, J. C., Da Silva, S. N., Peixoto, R. A. F., Carvalho, W., Castro, J., et al. (2016). Mortars for laying and coating produced with iron ore tailings from tailing dams. *Construction and Building Materials, 112*, 988–995. https://doi.org/10.1016/j.conbuildmat.2016.03.027.

Grant, W. (2019). Brazil's Barão de Cocais waits as dam nearby at risk of collapse. Retrieved 23 November 2019 from https://www.bbc.com/news/world-latin-america-48391767.

Guerra, M. B. B., Teaney, B. T., Mount, B. J., Asunskis, D. J., Jordan, B. T., Barker, R. J., et al. (2017). Post-catastrophe analysis of the Fundão tailings dam failure in the Doce River system, southeast Brazil: Potentially toxic elements in affected soils. *Water, Air, and Soil Pollution, 228*(7), 252. https://doi.org/10.1007/s11270-017-3430-5.

Inamuddin, & Luqman, M. (2012). *Ion exchange technology I. Theory and materials*Dordrecht: Springer Netherlands. https://doi.org/10.1007/978-94-007-1700-8.

Izidoro, J. de C. (2013). *Síntese e caracterização de zeólita pura obtida a partir de cinzas volantes de carvão.* University of Sao Paulo.

Izidoro, J.de C., Fungaro, D. A., Abbott, J. E., & Wang, S. (2013). Synthesis of zeolites X and A from fly ashes for cadmium and zinc removal from aqueous solutions in single and binary ion systems. *Fuel, 103*(September), 827–834. https://doi.org/10.1016/j.fuel.2012.07.060.

Izidoro, J.de C., Fungaro, D. A., Dos Santos, F. S., & Wang, S. (2012). Characteristics of Brazilian coal fly ashes and their synthesized zeolites. In: *Fuel Processing Technology, 97*, 38–44. https://doi.org/10.1016/j.fuproc.2012.01.009 January 2011.

Izidoro, J.de C., Fungaro, D. A., & Wang, S. B. (2011). Zeolite synthesis from Brazilian coal fly ash for removal of Zn2+ and Cd2+ from water. *Advanced Materials Research,* 356–360. June 2014, 1900-1908 https://doi.org/10.4028/www.scientific.net/AMR.356-360.1900.

Izidoro, J.de C., Miranda, S., Guilhen, S. N., Fungaro, D. A., & Wang, S. (2018). Treatment of coal ash landfill leachate using zeolitic materials from coal combustion by-products. *Advanced Materials and Technologies for Environmental Applications, 2*(1), 177–186.

Jackson, E. (1986). *Hydrometallurgical extraction and reclamation* (1st ed.). Southampton: Ellis Horwood Limitedhttps://doi.org/10.1016/0304-386X(87)90057-0.

Labonne, B. (2016). Mining dam failure: Business as usual? *Extractive Industries and Society, 3*(3), 651–652. https://doi.org/10.1016/j.exis.2016.03.010.

Liu, R., & Poon, C. (2016). Effects of red mud on properties of self-compacting mortar. *Journal of Cleaner Production, 135*, 1170–1178. https://doi.org/10.1016/j.jclepro.2016.07.052.

Luz, A. B. da, Sampaio, J. A., & França, S. C. A. (2010). *Tratamento de minérios. CETEM (5ª edição, Vol. 1* (Rio de Janeiro).

Mallapur, V. P., & Oubagaranadin, J. U. K. (2017). A brief review on the synthesis of zeolites from hazardous wastes. *Transactions - Indian Ceramic Society, 76*(1), 1–13. https://doi.org/10.1080/0371750X.2016.1231086.

Marta-Almeida, M., Mendes, R., Amorim, F. N., Cirano, M., & Dias, J. M. (2016). Fundão Dam collapse: Oceanic dispersion of River Doce after the greatest Brazilian environmental accident. *Marine Pollution Bulletin, 112*(1–2), 359–364. https://doi.org/10.1016/j.marpolbul.2016.07.039.

Petrov, I., & Michalev, T. (2012). Synthesis of zeolite A: A review. *Semantic scholar*. (51, Book 9.1: 30–35). Retrieved 23 November 2019 from http://conf.uni-ruse.bg/bg/docs/cp12/9.1/9.1-5.pdf.

Santamarina, J. C., Torres-Cruz, L. A., & Bachus, R. C. (2019). Why coal ash and tailings dam disasters occur. *Science, 364*(6440), 526–528. https://doi.org/10.1126/science.aax1927.

Segura, F. R., Nunes, E. A., Paniz, F. P., Paulelli, A. C. C., Rodrigues, G. B., Braga, G.Ú. L., et al. (2016). Potential risks of the residue from Samarco's mine dam burst (Bento Rodrigues, Brazil). *Environmental Pollution, 218*, 813–825. https://doi.org/10.1016/j.envpol.2016.08.005.

Wibowo, E., Rokhmat, M., Sutisna, K., & Abdullah, M. (2017). Reduction of seawater salinity by natural zeolite (Clinoptilolite): Adsorption isotherms, thermodynamics and kinetics. *Desalination, 409*, 146–156. https://doi.org/10.1016/j.desal.2017.01.026.

Zagorodni, A. A. (2012). *Ion exchange materials: Properties and applications, Vol. XXXIII*Stockholm: Elsevierhttps://doi.org/10.1007/s13398-014-0173-7.2 First edit.